J. Bangladesh Acad. Sci. 45(1); 73-83: June 2021 DOI: 10.3329/jbas.v45i1.54261

Journal of Bangladesh Academy of Sciences

Journal homepage: http://www.bas.org.bd/publications/jbas.html

Research Article

The effect of flight state parameters on the performance of photovoltaic modules in solar aircraft

Saydul Morshed Tanvir[1], Xiao Wenbo[1]*, Jin Xin[1]

Key Laboratory of Nondestructive Testing, Ministry of Education, Nanchang Hangkong University, Nanchang, Jiangxi, China

ARTICLE INFO

Article History

Received: 30 April 2021

Revised: 08 June 2021

Accepted: 09 June 2021

Keywords: Solar aircraft, Photovoltaic modules, Flight parameters, Photovoltaic cell performance, Performance prediction.

ABSTRACT

Based on the power generation model of photovoltaic modules, the effects of flight speed, altitude, time and area in solar aircraft on the performance of photovoltaic modules have been studied. As the flight speed increases, the power generated by the module increases but tends to saturate. When the conversion efficiency of photovoltaic modules is improved, the required power of the solar aircraft and the power generated by the photovoltaic modules are balanced at a faster flight speed. The power generated by the modules increases with the flight altitude but tends to saturate due to the drop of air temperature and the surface temperature of the module. The higher the altitude, the smaller is the atmospheric density, and atmospheric permeability, and the greater is the solar radiation intensity, and thus the power generated by the module increases. The power generated by the components is the strongest at noon. Battery performance is the strongest in summer and the weakest in winter, as the module's performance is mainly determined by the intensity of solar radiation. Finally, the energy distribution of solar aircraft and long-time space flight has been discussed.

Introduction

Solar-powered aircraft have attracted significant attention owing to their potential for long-endurance flight and broad application. Therefore, long-term and high-altitude emplacement of solar aircraft is one of the leading research directions in recent years (Zhang et al., 2019). The performance of photovoltaic modules in solar aircraft is influenced by a range of parameters such as flight speed, altitude, time, and area, and so on. In addition to the solar radiation intensity and the external temperature (Rajendran and Smith, 2018; Wu et al., 2019) and the solar altitude angle, the power generation of the components on the solar aircraft is related to the solar radiation intensity and the external temperature. In fact, as the flight speed, altitude, time, and area of the solar aircraft change, the ambient air temperature, solar radiation intensity, air density, and other environmental factors around the aircraft also change. These factors are coupled together to affect the performance of the components installed on the aircraft (Ahn and Ahn, 2019, Oettershagen, 2017). Therefore, based on the power generation model of the photovoltaic module, the research has been focused on the simulation of cell performance characteristics

*Corresponding author:<saydul.tanvir@yahoo.com (SMT); wbxiao@semi.ac.cn (XW)>

[1]Jiangxi Engineering Laboratory for Optoelectronics Testing Technology, Nanchang Hangkong University, Nanchang, Jiangxi, China, 330063

with the flight state parameters. The general execution of independent photovoltaic frameworks relies upon the degree of sun-oriented irradiance and the battery's charge status. The outcomes show additionally spread purchase load irrespective of the degree of sunlight-based irradiance. In this simulation, clear sky and overcast sky, and spring-pre-winter day conditions have been used. The power generation model of the photovoltaic module is based on four important elements such as flight speed, altitude, time, and the area, which affect solar aircraft on the performance of photovoltaic modules. Two specific objects: the monocrystalline silicon module and the solar aircraft, have been used. Due to the particularity of the energy system, flight strategy optimization is a significant way to enhance flight performance for solar-powered aircraft. The study will provide a knowledge base for the energy distribution of solar aircraft and long-time space flight.

Power generation model of photovoltaic module P_{solar}

The power generated by photovoltaic modules in the solar aircraft is related to the photoelectric conversion efficiency of photovoltaic modules on the wing, the solar radiation intensity received, and the area of photovoltaic modules laid on the aircraft. It can be shown as

$$P_{solar} = \eta G S \tag{1}$$

Equation (1) represents a classical model of photovoltaic modules and is widely used. Many studies have compared the theoretical data with the experimental data using this model and verified the accuracy (Dwivedi et al., 2018; Wilkins et al., 2009; Lee and Yu, 2017; Gao et al., 2013). The cell efficiency η is affected by photovoltaic cell type, and the surface temperature of photovoltaic modules T; and T is affected by aircraft operating conditions (flight speed, altitude, etc.). The light intensity G is related to the flight altitude, area, etc. S is associated with the size of the aircraft, which affects the total power of the aircraft.

Influence on photoelectric conversion efficiency η

Wu model is the most accurate model used for subsequent research. Wu model is represented by eq. (2), which is called model 1 (Wu et al., 2018).

$$\eta = \left[1 + (T - 25)\alpha_\eta\right]\eta^{\mathrm{STC}} \tag{2}$$

In eq. (2), α_η is the temperature correction coefficient; η^{STC} is the conversion efficiency at normal state ($1000\ \mathrm{Wm}^{-2},\ 2.5\mathrm{AM},\ 25°\mathrm{C}$).

Influence on the surface temperature of photovoltaic module T

Under the influence of solar radiation intensity (Wu et al., 2018), considered the influence of solar radiation intensity on the heat exchange of photovoltaic modules (Ran et al., 2007; Meral and Dincer, 2011; Cowtan et al., 2015); and established the convection heat exchange relationship between modules and the surrounding environment as shown in eq. (3)

$$\alpha \mathrm{G} = \eta \mathrm{G} + \varepsilon\sigma\left(T^4 - T_{\mathrm{sky}}^4\right) + h\left[T - \left(T_{\mathrm{atm}} + (\mathrm{NOCT} - 20)\frac{\mathrm{G}}{800}\right)\right] \tag{3}$$

In eq. (3), the left side is the solar energy that can be directly obtained by the photovoltaic module, α is the absorption rate of the component. In the equation, the right side is the energy converted by the components and the energy lost by the convection between the components and the outside (including the heat exchange with the outside atmosphere and the

heat exchange with the flowing air). Where ε is the thermal radiation impassivity of the component, is 0.85; σ is Boltzmann constant, $\sigma = 5.67 \times 10^{-8}\mathrm{Wm^2K^{-4}}$, T_{sky} ($\mathrm{T_{sky}} = 0.0552\mathrm{T_a^{1.5}}$, T_{a} is the surface temperature of the area) is the effective sky temperature; h is the convective heat transfer coefficient; T_{atm} atmospheric temperature corresponding to different heights. Convective heat transfer coefficient in eq. (3), h is related to flight speed, air thermal conductivity, etc. which can be expressed as:

$$h = \frac{\lambda_{air} N_u}{c} \tag{4}$$

In eq. (4), λ_{air} is the thermal conductivity of air, by 0.024; c is a wing string; N_u is the Nusselt coefficient

$$\mu_{\mathrm{air}} = \left(\frac{T_{sky}}{288.15}\right)^{1.5} \frac{288.15 + 110.4}{T_{sky} + 110.4} \mu_o \tag{5}$$

$$N_u = \begin{cases} 0.664 Re^{0.5} \left(\frac{c_p \mu_{air}}{\lambda_{air}}\right)^{\frac{1}{3}}; & Re \le 5 \times 10^5 \\ (0.034 Re^{0.8} - 871) \left(\frac{c_p \mu_{air}}{\lambda_{air}}\right)^{\frac{1}{3}}; & Re > 5 \times 10^5 \end{cases} \tag{6}$$

In eq. (5), $Re = \frac{\rho(z)V}{\mu_{air}}$ Reynolds number; $Pr = \frac{c_p \mu_{air}}{\lambda_{air}}$ is the Planck number; $\rho(z)$ is the atmospheric density corresponding to different heights; V is the velocity of air flowing on the surface of the upper assembly of the wing; c_p is the specific heat capacity of air at constant pressure, is 1.004; μ_{air} is the air viscosity coefficient, as shown in eq.(6); μ_o is the viscosity coefficient of dry air at 25 ℃, which is 17.6×10^{-6}.

$$T_{atm} = T(b) + l(b)[z - z(b)] \tag{7}$$

In eq. (7), b represents a certain layer, $T(b)$is the temperature of the starting point in the atmosphere of this layer if the flight altitude is at the first layer $T(b) = T_a$; $l(b)$ is the temperature change rate of the layer, $z - z(b)$ is the height difference between the point and the starting point of the layer. The starting point of each atmosphere (m): $[0,\ 11000,\ 20000,\ 32000,\ 47000,\ 51000,\ 71000,\ 84852]$. Temperature change rate of each layer of atmosphere $l(b) = [-0.0065,\ 0,\ 0.0010,\ 0.0028,\ 0,\ -0.0028 - 0.0020,\ 0]$.

The T was estimated as follows: available from meteorological data T_a and T_{sky}; substituting flight altitude into equation (7) can calculate the corresponding T_{atm}, Flight speed V and T_{sky} Substituting equation (4) to equation (6) can obtain the convective heat transfer coefficient h; Finally, we know T_{sky}, T_{atm} and h, from equation (3), it can be calculated that the T, take T in (2) to get η.

Solar radiation intensity G

G is not only affected by time, region, and other factors but also by atmospheric permeability, atmospheric density, and other factors. It can be expressed as follows (Ran et al., 200; Mghouchi et al. 2016):

$$G = G_o D_z \sin A \tag{8}$$

Where G_o, the solar radiation intensity outside the atmosphere is $1353\mathrm{Wm^{-2}}$; $\mathrm{D_z}$ is the air permeability; A it is the solar altitude angle with the photovoltaic module of the solar aircraft wing as the plane; although there is an arc on the wing surface

The calculation is as follows:

$$\sin \mathrm{A} = \cos\delta \cos\phi \cos\omega + \sin\delta \sin\phi \tag{9}$$

Where, ϕ is the latitude of the area where the aircraft is located; $\delta = 23.45 \sin\left[\frac{360}{365}(284 + d_n)\right]$ is the declination angle of the area. d_n is the number of days between the date of flight and January 1; $\omega = 15^{o}.(12 - t)$ is the time angle of the sun (t for the time of flight, such as 10 a.m., then $t = 10$).

Air permeability of solar aircraft at flight altitude is D_z. From equations (10) to (13), in (12) m is the air quality at a specific place (Panagiotou et al., 2016); equation (13) is atmospheric pressure $p(z)$ for the relationship with the flight altitude, in equation (12) $p(0) = 101.3\text{kPa}$. Thus, atmospheric density $\rho(z)$ the relationship with atmospheric pressure is $\rho(z) = \frac{p(z)M}{RT_{atm}}$.

$$D_z = 0.5\left(e^{-0.65\text{m(z,A)}} + e^{-0.095\text{m(z,A)}}\right) \quad (10)$$

$$m(z = 0, A) = \sqrt{1229 + (614 \sin A)^2} - 614 \sin A \quad (11)$$

$$m(z, A) = m(0, A)\left[\frac{p(z)}{p(0)}\right] \quad (12)$$

$$p(z) = e^{5.25885 \times \ln(288.15 - 0.0065z) - 18.2573} \quad (13)$$

G was estimated as follows. First, the flight date difference d_n and flight time t bring in declination angle respectively δ and solar hour angle ω formula, get δ and ω; Second, we will find δ, ω and the latitude of the area where the aircraft is located δ. Third, the sine of the time angle of the sun can be calculated by using equation (9). Then, the air permeability can be calculated by substituting the flight altitude into equation (10) to equation (13). Finally, according to equation (8), the solar radiation intensity that a solar aircraft can receive at a fixed time, a fixed area and a selected flight altitude can be obtained G.

Power required by aircraft under different flight parameters

To ensure the minimum power consumption during normal operation of solar aircraft, in addition to changing the flight attitude when changing the flight altitude, most of the time is level flight. When solar energy flies at different speeds, the required level of flight power is different. The calculation is made using (Torabi et al., 2011):

$$P_p = \frac{1}{2}\rho(z)V^3 S C_{D_o} + \frac{2kW^2}{\rho(z)VS} \quad (14)$$

In eq. (14), P_p is the level flight power required for solar-powered aircraft; C_{D_o} is the zero-lift drag coefficient; W is the gravity of the aircraft; k is the proportionality constant, calculated as follows (Torabi et al., 2011; Shiau et al., 2010):

$$k = \frac{4}{3}\frac{1}{\pi u AR} \quad (15)$$

$$u = 1.78(1 - 0.045\ AR^{0.68}) - 0.64 \quad (16)$$

$$W = L = \frac{1}{2}\rho(z)V^2 S C_L \quad (17)$$

In eq. (15), AR is the aspect ratio, and u is the Oswald efficiency factor. The aspect ratio is 7; the area of photovoltaic modules on the wing S by 4.91m^2; C_D by 0.00758; type (17) in C_L. The lift coefficient is 0.5805; Other parameters are as above.

When the plane is in level flight, the lift (L) is equal to the gravity (W); P_p is only the power required for the horizontal flight of the solar aircraft. However, in the actual flight, because the efficiency of the motor and propeller is certain, the power demand of the actual aircraft is greater; the power required for the actual

flight of the aircraft $P_{require}$. The calculation is as follows (Torabi et al., 2011):

$$P_{require} = \frac{P_p}{\eta_m \eta_p} \quad (17)$$

In equation (18), η_m is the working efficiency of the motor; η_p working for the efficiency of the propeller, for 0.8.

When the flight altitude of the solar aircraft is constant, the atmospheric density in equation (14) is affected by the flight altitude, and other aircraft parameters remain unchanged. Therefore, by changing the flight speed of the aircraft v, the power required by the aircraft at different flight speeds can be calculated.

Results and Analysis

Flying speed and height

Flight parameters or Boundaries have an impact on the possible visualizations and the general flight path.

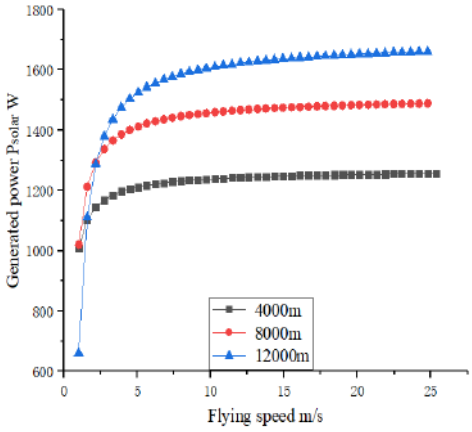

Fig. 1. The power generated by photovoltaic modules at different flying heights and flight speeds.

Consequently, it is imperative to acknowledge what goes into every one of these boundaries and what one has to keep an eye out for a while choosing them. In this case, flight altitude parameters are $\eta^{STC} = 0.13$, $V = 15 ms^{-1}$, given the current data we are dealing with. Other parameters are the same as in section 1. The power generated by photovoltaic modules at $0 - 30\ ms^{-1}$, respectively, in the flight altitude range of $4000\ m, 8000\ m, and\ 12000\ m$, respectively, is shown in Fig. 1.

At low speed, induced power increases sharply and linearly. Between $3\ ms^{-1}$ to $7\ ms^{-1}$, we observe knee points. In this region, generated power tends to attain a limiting value from the linear region. After the knee point, the graph maintains an almost constant value. This is the saturation region.

With an increase in flying height, each graph operates with higher power levels. At a lower height ($4000\ m$), the graph attains a limiting value with a lower speed, whereas; at a higher height, the graph gets flooded with a higher rate. There is still an increasing trend/slope in the saturation region. This slope is more prominent with higher heights. The power generation of the solar aircraft components is related to solar radiation intensity and external temperature. Flying speed impacts temperature, whereas flying height impacts both solar radiation intensity and external temperature. When the flight speed increases, the power generated by the module increases but tends to saturate. The reason is that the speed increase will effectively reduce the surface temperature of the module, but the improvement of the performance is limited. The power generated by the modules increases with the flight altitude but tends to saturate. The reason is that the air temperature drops, and the surface temperature of the module drops when the flight altitude rises. Simultaneously, the higher the altitude, the smaller is the

atmospheric density and atmospheric permeability, and the greater is the solar radiation intensity. Thus, the power generated by the module increases. The saturation is due to the performance limitations of the component itself.

In fact, in high-altitude areas, the air is thinner, the heat transfer coefficient should be reduced, and the atmospheric temperature tends to stabilize. Therefore, the temperature of the photovoltaic cell will approach a fixed value as the flight altitude increases, and the improvement in the performance of the photovoltaic cell is limited. The generated power will not change from a value of around 600 W to 1600 W at an altitude of 12000 m for a speed varying from 2 m/s to 25 m/s. In addition, we found that when the wind speed is above 5 m/s, the model gives a relatively accurate prediction result, namely, the results are satisfactory at higher speeds. Generally speaking, we provide a theoretical prediction of the trend here.

Power require

If the sky is clear and cloudless, take Dhaka as an example, the latitude is $23.77°n$; flight time $t = 6$ a. m. Surface temperature T_a is 15℃; the flight altitude is 8 km. The power generated by photovoltaic modules and the power required by aircraft varies with flight speed when the standard conversion efficiencies are $0.13,\ 0.16,\ 0.19, and\ 0.22$, respectively, as shown in Figure 2. The estimation of the recuperation factor may be affected by the position of the thermometer on the airplane. Preferably, thermometers should be mounted with their admissions outside the limit layer, in a zone unaffected by an isolated stream of releases from the aircraft (for example, close to fuel or cooling - air vents) where the nearby Mach number is equivalent to the free stream Mach number.

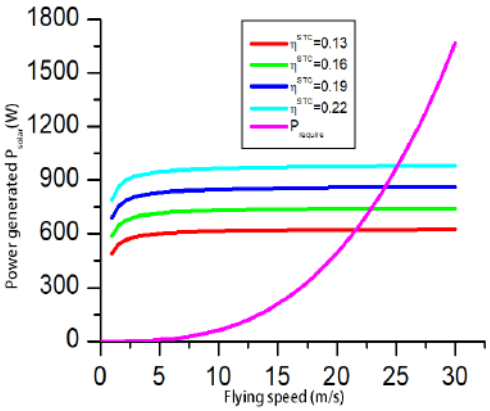

Fig. 2. The power generated by photovoltaic modules at conversion efficiency by the aircraft change with the flight speed.

Frequently, this implies that they should be mounted spot on of the airplane. At supersonic velocities, the demonstrated temperature rise is achieved in two stages, the ascent through the stunning wave at section to the thermometer and the upgradation compared to the recuperation factor of the thermometer. For example, the air entering the thermometer is now at a higher static temperature than the free stream esteem, yet a subsonic Mach number.

Figure 3 shows the 'Energy Balance' point of the aircraft increases at 520.958 W, 646.707 W, 772.455 W, and 889.222 W with the rise of standard conversion efficiency η^{STC} from $0.13, 0.16, 0.19, and\ 0.22$, respectively.

Energy Balance takes place between the power generated by the modules and the power required by the aircraft. Mathematically, Energy Balance = power generated P_{solar} − power required P_{req}. With increasing η^{STC}, generated power also increases by equations 1 and 2. But, the power required P_{req} does not

vary with η^{STC}. So, energy balance $\alpha\ \eta^{STC}$ ... . (equation 1,2) varies as shown in Fig. 3.

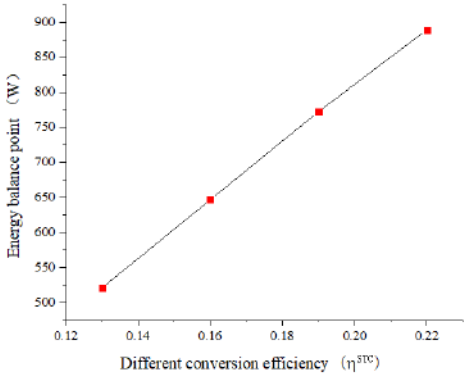

Fig. 3. The Energy Balance at a different standard conversion efficiency

This positive slope of the graph indicates that the aircraft will work at a higher Energy Balance with higher η^{STC}. Or in other words, with increasing efficiency η^{STC}, P_{solar} will be at a higher level. So, to achieve the energy balance point, P_{req} will cut the P_{solar} curve by moving right. This tendency of moving directly or "moving backward" is explained by equation 1. Thus, if the battery efficiency is increased, the energy balance point will move backward to select more flight speeds.

From Figure 4, it can be seen that the flying speed of the aircraft (at which 'Energy Balance' occurs) increases at $20.4484\ ms^{-1}, 21.9283\ ms^{-1}, 23.2735\ ms^{-1}$ and $24.3498\ ms^{-1}$, with the increase of standard conversion efficiency η^{STC} from 0.13, 0.16, 0.19, *and* 0.22, respectively.

Energy Balance = power generated P_{solar} – power required P_{req}. Now, $P_{solar}\alpha\eta^{STC}$ and $P_{req}\alpha$ flying speed.

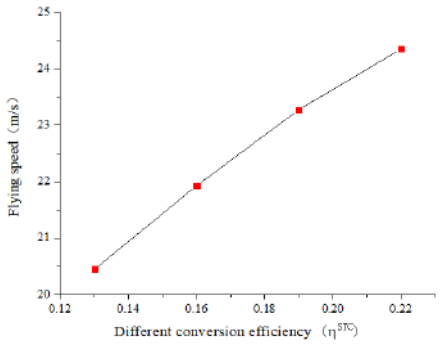

Fig 4. Flying speed (at energy balance point) vs. different standard conversion efficiency.

At energy balance point, $P_{solar} = P_{req}$ and Energy Balance $= 0$. So, at the energy balance point, $P_{req} = P_{solar}$.

Flying speed $= K\eta^{STC}$ [K =proportionality constant]

This positive slope of the graph indicates that it can operate at a higher-flying speed with higher η^{STC}. The graph is piecewise linear because it has a lower slope (after $\eta^{STC} = 0.19$) than the left part of it.

Energy balance $\alpha\eta^{STC}$ and Flying speed $= K\eta^{STC}$.

So, flying speed α is energy balance. That means, if energy balance is achieved at a higher level of generated Power (P_{solar}), the aircraft can work at a higher-flying speed**.**

Flight time

Flight parameters or boundaries have an impact on the possible visualizations and the general flight path. It is, consequently, imperative to acknowledge what goes into every one of these boundaries and what one has to keep an eye out for a while choosing them, $\eta^{STC} = 0.13$, $V = 15ms^{-1}$.

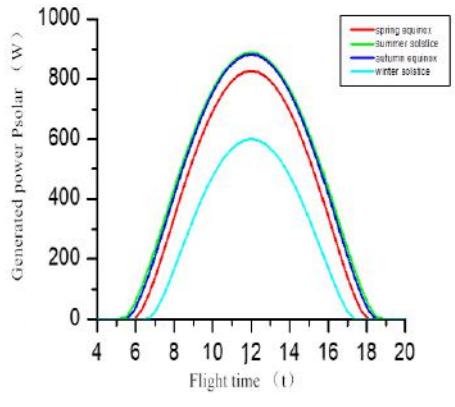

Fig. 5. The power generated by photovoltaic modules in the spring equinox, summer solstice, autumn equinox and winter solstice.

The surface temperature of the spring equinox, summer solstice, autumn solstice, and winter solstice T_a $24, 35, 32\ and\ 15℃$ respectively. Other parameters are the same. The power generated by photovoltaic modules in a day in spring equinox, summer solstice, autumn solstice, and winter solstice is shown in figure 5.

Fig. 5 shows the power change of photovoltaic modules in the spring equinox, summer solstice, autumn equinox, and winter solstice calculated according to formula (1), where the flight time is 4 a.m. to 8 p.m. As can be seen from Figure 5, the power generated by the components under the four solar terms gradually rises to a peak value and then declines; the peak value is about noon. It can be seen that the flight time mainly affects the solar radiation intensity and the external atmospheric temperature of the photovoltaic modules in the aircraft. The solar radiation is the strongest at noon, and the atmospheric temperature is also the highest, so the power is approximately symmetrical around the peak of 12. It is noted that the power generated by the components of the spring equinox, summer solstice, autumn equinox, and winter solstice is 827.718 W, 892.484 W, 884.712 W, and 602.338 W, respectively. This is different, with the highest in summer and the lowest in winter; the reason is that the solar radiation of summer solstice is the strongest, and the solar radiation of the winter solstice is the smallest. We can see from eq. (1) that the power of the solar cell is affected by the solar radiation intensity G. So the stronger the G, the stronger the solar cell power. The solar radiation in summer is very close to that in autumn, so the power in summer is very similar to that in autumn. The solar radiation intensity in spring and winter is smaller than that in the other two seasons, so the power is smaller. The solar radiation intensity in winter is the least, so the power is also the least. The variation of solar radiation intensity in a year is the same as the variation of solar cell power, as seen in Fig. 6.

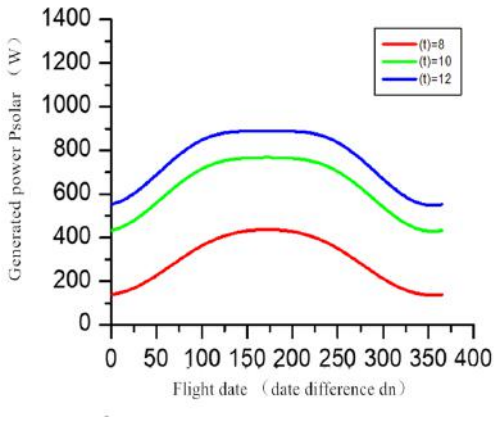

Fig. 6. The power generated by photovoltaic modules during one-year at 8:00, 10:00, and 12:00 noon on day one.

According to Figure 6., the power generated by the photovoltaic modules during the annual flight time at $8{:}00, 10{:}00, and\ 12{:}00\ noon$ using these two selected periods from the data, we can make our observations and subsequent

analysis. In the whole year, the solar radiation intensity is significant in summer, and the atmospheric temperature is the highest. Therefore, the power generated by the module is symmetrical around the summer solstice. It is noted that under the influence of solar radiation intensity, the power generated at $t = 8$ is the smallest, and at $t = 12$ is the largest. The above output characteristics are mainly because the solar radiation intensity primarily determines the module's performance.

Flight area

Except for the latitude of the flight area ϕ parameter, $\eta^{STC}0.13,\ and\ V = 15\ ms^{-1}$, the other parameters are the same as those in Section 1. Thus, the condition is the variation of the power of the photovoltaic module when the latitude of the flight area changes, as shown in Fig.7.

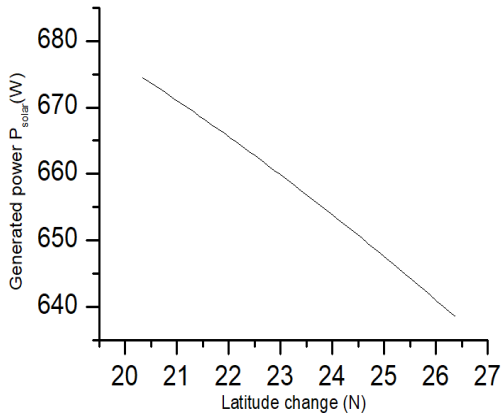

Fig. 7. Power generated by photovoltaic modules as latitude changes.

Figure 7 shows the power generated by photovoltaic modules in the latitude range of $20.34°\ n\ to\ 26.38°\ n$ in Bangladesh. We can see that, with the increase of latitude, the less power the aircraft photovoltaic modules produce. The latitude changes of the aircraft area according to eq. (9) will affect the solar radiation intensity in eq. (8), which will lead to the power change of components in eq. (1). So, the higher the latitude is, the smaller the solar altitude angle is, and the smaller the solar radiation can be received by the photovoltaic module, which leads to the degradation of the module performance.

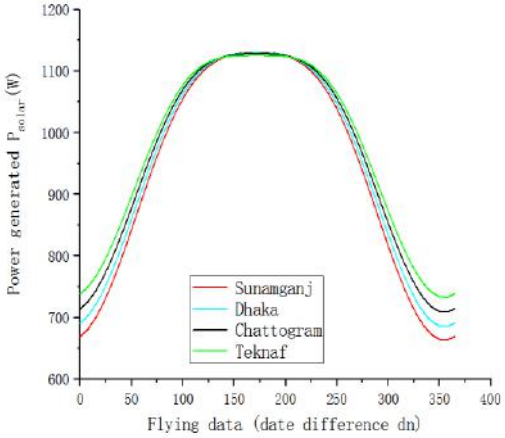

Fig, 8. The power generated by photovoltaic modules at Sunamganj, Dhaka, Chattogram and Teknaf in one year.

Figure 8 shows the power generated by four urban components in Sunamganj, Dhaka, Chattogram, and Teknaf in one year. The latitudes of the four urban centers are 25.08°, 23.77°, 22.35°, and 20.85° respectively, and the latitudes decrease in turn. The aircraft photovoltaic modules in Sunamganj have the lowest power generation, while the Teknaf modules have the strongest power. According to Fig. 7, the lower the latitude is, the smaller the power variation generated by the components is, and the larger the total power generated is; the higher the latitude is. As a result, the lower the latitude is, the more favorable it is for the flight of solar-powered aircraft. From Figures 5-8, it is therefore conclusive that the performance of photovoltaic modules is mainly affected by the solar radiation intensity G.

Conclusion

Based on the power generation model of photovoltaic modules, this paper studies the parameters that affect the performance of modules in the solar aircraft, such as flight speed, altitude, time, and area. The conclusions are as follows:

a. The power generated by the modules increases with the flight altitude, but tends to saturate. The reason is that the air temperature drops, and the surface temperature of the module drops when the flight altitude rises. At the same time, the higher the altitude, the smaller the atmospheric density and atmospheric permeability are, and the greater the solar radiation intensity is, and thus, the power generated by the module increases. The reason for saturation is the performance limitations of the component itself.

b. As the aircraft speed increases, the power generated by the components increases but tends to be saturated. The reason is that the increase of speed effectively reduces the surface temperature of components, but the performance improvement is limited. The power required by the aircraft increases exponentially with the increase of speed. There is an energy balance between the power generated by the components and the power required by the aircraft. With increasing efficiency η^{STC}, P_{solar} will be at a higher level. So, to achieve the energy balance point, P_{req} will cut the P_{solar} curve by moving right. If the battery efficiency is increased, the energy balance point will move backward to select more flight speeds. If energy balance is achieved at a higher level of generated Power (P_{solar}), the aircraft can work at a higher-flying speed**.**

c. The effect of flight time on the performance of photovoltaic modules is obvious. In a day, the power generated by the components is approximately symmetrical around the sun at 12 noon with the strongest at noon. The performance of a medium battery is the strongest in summer and the weakest in winter. The reason is that the performance of the module is mainly determined by the solar radiation intensity.

With the increase of latitude, the power generation of components is smaller. The reason is that the higher the latitude is, the smaller the solar altitude angle is, and the smaller the solar radiation the photovoltaic modules can receive. In addition, by comparing the power generated by components in Dhaka, Sunamganj, and other two regions in one year, it can be seen that the lower the latitude is, the higher the total power generated by components is, and the more stable the performance of components is in one year; the higher the latitude is, the greater the performance fluctuation of components is, and the smaller the total power generated. Therefore, the low latitude area is more suitable for solar aircraft flight.

Acknowledgments

This work was supported in part by the National Natural Science Foundation of China under Grant No. 12064027, by Open Fund of the Key Laboratory of Nondestructive Testing of Ministry of Education of Nanchang Hong Kong University under Grant Nos. EW201908442 and EW201980090.

References

Ahn HJ and Ahn J. Design and analysis of a solar-power mini-uav for extended endurance at low altitude. *Int. J. Aeronaut. Space Sci.* 2019; 20: 561-569.

Cowtan K, Hausfather Z, Hawkins E, Jacobs P, Mann ME, Miller SK, Steinman BA, Stolpe MB and Way RG. Robust comparison of climate models with observations using blended land air and ocean sea surface temperatures. *Geophy. Res. Lett*. 2015; 42: 6526–6534.

Dwivedi VS, Kumar P, Ghosh AK and Kamath GM. Selection of size of battery for solar powered aircraft. *IFAC-Papers* Online; 2018; 51(29): 424-430.

Gao XZ, Hou ZX, Guo Z, Liu JX and Chen XQ. Energy management strategy for solar-powered high-altitude long-endurance aircraft. *Energy Convers. Manag*. 2013; 70: 20–30.

Lee JS and Yu KH. Optimal path planning of solar-powered UAV using gravitational potential energy. *IEEE Trans. Aerosp. Electron. Syst.* 2017; 53(3): 1442-1451.

Meral ME and Dincer F. A review of the factors affecting operation and efficiency of photovoltaic based electricity generation systems. *Renew. Sustain. Energy Rev.* 2011; 15(5): 2176-2184.

Mghouchi YE, Bouardi AE, Choulli Z and Ajzoul T. Models for obtaining the daily direct, diffuse and global solar radiations. *Renew. Sustain. Energy Rev.*2016; 56: 87–99.

Oettershagen P. High-fidelity solar power income modeling for solar-electric UAVs: Development and flight test based verification. *Tech. Report.* 2017; 1703:07385.

Panagiotou P, Tsavlidis I and Yakinthos K. Conceptual design of a hybrid solar MALE UAV. *Aerosp. Sci. Technol.* 2016; 53: 207-219.

Rajendran P and Smith H. Experimental study of solar module maximum power point tracking system under controlled tempe-rature conditions. *Int. J. Adv. Sci. Eng. Inf. Technol.* 2018; 4(8): 1147-1153.

Ran HJ, Thomas R and Mavris DA. Comprehensive global model of broadband direct solar radiation for solar cell simulation. *45th AIAA Aerospace Sciences Meeting and Exhibit 8-11 January 2007, Reno, Nevada*; AIAA 2007-33.

Shiau JK, Ma DM and Chiu CW. Optimal sizing and cruise speed determination for a solar-powered airplane. *J. Aircr*. 2010; 2(47): 622-629.

Torabi HB, Sadi M and Vatjani AY. Solar power system for experimental Unmanned Aerial Vehicle (UAV); Design and Fabrication. *2011 2nd Power Electronics, Drive Systems and Technologies Conference;* 2011. p. 129-134.

Wilkins G, Fourie D and Meyer J. Critical design parameters for a low altitude long endurance solar powered UAV. *IEEE AFRICON*; 2009.

Wu MJ, Shi ZW, Xiao TH and Ang HS. Energy optimization and investigation for Z-shaped sun-tracking morphing-wing solar-powered UAV *Aerosp. Sci. Technol.* 2019; 91: 1–11.

Wu JF, Wang HL, Huang Y, Su ZK and Zhang MH. Energy management strategy for solar-powered UAV long-endurance target tracking. *IEEE Trans. Aerosp. Electron. Syst.* 2018; 13(1): 1878-1891.

Zhang WW, Zhang LG, Yan ZW and Wang L. Structural Design and Difficulties of Solar UAV; In: Proceedings of the *IOP Conference Series: Materials Science and Engineering: 3rd International Conference on Aeronautical Materials and Aerospace Engineering (AMAE 2019) 24–26 May 2019, Shanghai, China*; 2019; 608: 01201.